IMPACT OF ORGANIC RANKINE CYCLE WORKING FLUID SELECTION ON HEAT EXCHANGER DESIGN AND COST

Leighton Taylor[1], Sandeep Siwach[2], and Susan Krumdieck[3]

[1,2,3] Mechanical Engineering, University of Canterbury, Private Bag 4800, Christchurch, 8100, New Zealand

[1]leighton.taylor@pg.canterbury.ac.nz
[2]sandeep.siwach@pg.canterbury.ac.nz
[3]susan.krumdieck@canterbury.ac.nz

Keywords: *Organic Rankine Cycle, Low Temperature Geothermal, Working Fluid Selection, Heat Exchanger Design and Costing*

ABSTRACT

The Organic Rankine Cycle (ORC) is used to convert low temperature heat into useable energy. Each ORC is a specifically tailored system and its design must take into account each aspect of the project, such as the resource available, size of the power plant, and the economics of the project. The working fluid selection is a critical design decision for an ORC as it influences the design of each of the components.

There are several different working fluids used in commissioned ORCs, the most common being N-Pentane. Non-flammable refrigerants such as R134a and R245fa are also used in small automated ORCs because of their reduced risk of explosion. R134a and R245fa are both HFC refrigerants with high global warming potentials that could potentially be phased out in the near future.

This paper uses thermodynamic models to investigate the impact of the working fluid on an ORC and further investigate the choice of working fluid on the design of the heat exchangers. The heat exchangers are a critical component for ORCs as they can contribute to at least 20% of the capital cost[1].

1. INTRODCUTION

1.1 Low Temperature Resources

Low temperature geothermal resources have not been utilized to the same extent as medium and high temperature geothermal reservoirs. Large geothermal systems utilizing medium or high temperature fluid typically use a steam cycle to generate electricity. In some situations the Organic Rankine Cycle (ORC) has also been used as a standalone system or alongside these steam cycles.

Recently there has been renewed interest in low temperature geothermal ORCs and a number of companies are providing smaller ORCs that can operate from a low temperature resource. Japan is an example of the new interest in low temperature ORCs; they are using hot springs and other low temperature geothermal resources to assist in meeting their renewable energy goals. A low temperature geothermal ORC generally has shorter setup times compared to large geothermal developments [2].

1.2 Organic Rankine Cycle

An ORC uses an organic fluid in place of water in a rankine cycle. The organic fluid facilitates use with a large range of resource temperatures as the organic fluid can boil at lower temperatures than water. Geothermal ORCs have used brine, steam, or a combination of brine and steam as the heat source for the ORC.

A basic ORC system has the following four main components: the feed pump provides the pressure increase and required mass flow rate, the pre heater and vaporizer heats the fluid from a sub-cooled liquid to either a saturated or superheated vapor, the expander produces usable work from the high pressure vapor, and a condenser cools the hot vapor back to a liquid state to repeat the cycle. An ORC also may have a recuperator to transfer heat from the hot vapor after the expander to the liquid fluid before the preheater. Figure 1 illustrates the components in a basic ORC.

The expander is critical to the success of an ORC and high performance ORCs use either an axial or radial turbine, as these have high isentropic efficiencies. A volumetric expander such as a scroll or screw expander can be a low cost alternative; however, often have reduced isentropic efficiency compared to turbines. The condenser for an ORC can be either air or water cooled. A water cooled condenser requires less space compared to an air cooled condenser, but requires a reliable year round water supply.

1.3 Working fluid selection

The working fluid in an ORC determines each state point of the thermodynamic cycle, the fluid flow rates, and the design of each component. Therefore, the working fluid selection is a critical design decision for an ORC [3].

Safety and availability must also be considered when selecting a working fluid. Hydrocarbons used in ORCs are flammable and pose an increased explosion risk which must be taken into account. Refrigerants which typically are not flammable can have greater environmental risks and some refrigerants have a high ozone depletion and global warming potential (GWP). Extra precautions must be taken to manage refrigerants with any severe environmental impacts.

The working fluids explored in this paper are N-Pentane, Isopentane, Isobutane, R245fa, and R134a. These fluids were chosen for their use in existing ORCs. Table one contains a list of the non-thermodynamic properties of each fluid as well as their use in commercial ORCs.

Table 1 - Working fluids investigated

Fluid	Flammable	GWP & life	Availability	Evidence
N-Pentane	Yes	20 – 5 Days	No Phase out plans	Ormat [4]
R245fa	No	1020 – 7.6 yrs	Still widely available; however, may be phased out in future	Purecycle – Raser [5]
R134a	No	1330 – 14.6 yrs		Purecylce – Chena [5]
Isopentane	Yes	11 – 5 Days	No Phase out plans	TAD ORC [6]
Isobutane	Yes	3.3 – 8 days	No Phase out plans	Otake Japan [7]

1.4 Heat exchangers

The heat exchangers are an important part of any ORC system as they facilitate the heat transfer between the hot fluid and the working fluid, and then again between the working fluid and the cooling fluid. The size of the heat exchangers is also used in the preliminary cost estimate of an ORC.

The heat exchangers investigated in this paper are of shell and tube type for the pre-heater and vaporizer. An air cooled condenser, which uses fans to blow air over banks of tubes containing the working fluid, is also considered for condensing the working fluid. Shell and tube heat exchangers are the industry standard for geothermal ORCs, where the geothermal fluid flows on the tube side and the working fluid is shell side. The air cooled condenser is also commonly used for geothermal ORCs that do not have a cooling water resource. Air cooled condensers (ACC) are also preferred in operations that need to maximize fluid returned to the reservoir. A traditional evaporative cooling tower requires makeup water and does not reinject 100% of the geothermal fluid.

Heat exchangers contribute a significant portion of the total ORC cost. Effective heat exchanger design can improve the performance of an ORC by minimizing the pinch points in the heat exchanger or reducing capital costs. This paper explores the impact working fluid properties have on heat exchanger design and whether the impact is sufficient to merit detailed heat exchanger design to assist with working fluid selection.

2. METHOD

An ORC model was developed to understand the implications of the selected working fluid on the heat exchanger design and cost. A low temperature geothermal ORC was modelled with two different brines temperatures, 130°C and 100°C. The geothermal fluid mass flow rate is adjusted to supply sufficient heat for a 250kW ORC.

2.1 ORC model

Figure 1 illustrates the common components in an ORC with the governing equations of each state point in table 2.

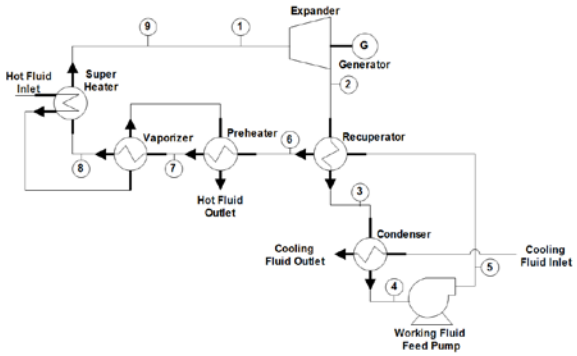

Figure 1 - Generic ORC plant diagram

The ORC modeled in this paper does not use a recuperator and only uses a superheater if the fluid has a wet saturation curve, which only applied to R134a. Superheating fluids reduces the risk of damaging the turbine but increases the size of the required heat exchanger.

The isentropic efficiency of the pump and the turbine was set to 85%. The pinch points in the heat exchangers were set to 15°C, a common rule of thumb for heat exchanger design [8]. Engineering equation solver (EES) was used to model the thermodynamics of the ORC. The evaporation temperature was determined from the pinch point and the brine temperature as the working fluid entered the preheater, which can be seen in Figure 2. The condensation temperature was determined from the pinch point of the cooling fluid and working fluid after de-superheating. The cooling fluid was designed to undergo a 30°C temperature rise to maintain a high condensing temperature, which is recommended to reduce the cost of the ACC[8]. This large temperature rise also allows for either a forced or induced draft air cooler.

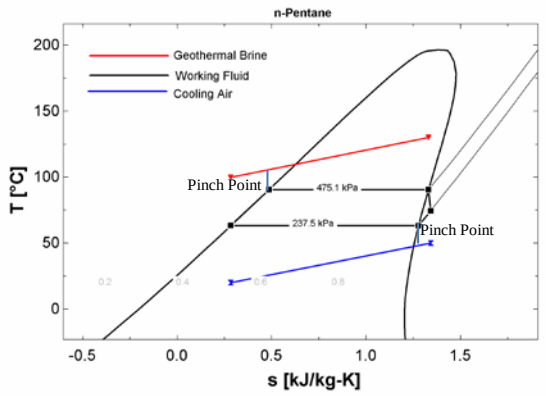

Figure 2 - T-S Diagram of the basic ORC model

The geothermal outlet temperature is determined from the enthalpy change required to preheat, vaporize, and if required super heat the fluid. The geothermal brine flow rate is determined by the required heat to guarantee the 250kW output.

Table 2 - Governing equations of the ORC model –
*** Recuperator not included in this ORC model –**
**** super heater only required for R134a**

Component	Governing Equations	
	Energy Balance	Isentropic or Transfer Efficiency
Expander **1-2** Superheated Vapor – Superheated Vapor	$W_{12} = \dot{m}(h_1 - h_2)$	$\eta_e = \frac{h_1 - h_2}{h_1 - h_{2s}}$
Recuperator – Desuperheat***2-3** Superheated Vapour – Saturated Vapour	$Q_{23} = \dot{m}(h_2 - h_3)$	$Q_{23} = U_r A_r \Delta T_{lm23}$
Condenser **3-4** Saturated Vapor – Saturated Liquid	$Q_{34} = \dot{m}(h_3 - h_4)$	$Q_{34} = U_c A_c \Delta T_{lm34}$
Pump **4-5** Saturated Liquid – Subcooled Liquid	$W_{45} = \dot{m}(h_5 - h_4)$	$\eta_p = \frac{h_{5s} - h_4}{h_5 - h_4}$
Recuperator* **5-6** Subcooled Liquid – Subcooled Liquid	$Q_{56} = \dot{m}(h_6 - h_5)$ $Q_{56} = Q_{23}$	$Q_{56} = U_r A_r \Delta T_{lm56}$ $Q_{56} = Q_{23}$
Pre-Heater **6-7** Subcooled Liquid – Saturated Liquid	$Q_{67} = \dot{m}(h_7 - h_6)$	$Q_{67} = U_{ph} A_{ph} \Delta T_{lm67}$
Vaporizer **7-8** Saturated Liquid – Saturated Vapor	$Q_{78} = \dot{m}(h_8 - h_7)$	$Q_{78} = U_v A_v \Delta T_{lm78}$
Superheater** **8-9** Saturated Vapor – Superheated Vapor	$Q_{89} = \dot{m}(h_9 - h_8)$	$Q_{89} = U_{sh} A_{sh} \Delta T_{lm89}$
Net Power	$W_{12} = W_{45} + Q_{56} + Q_{67} + Q_{78} + Q_{89} - Q_{23} - Q_{34}$	

2.2 Heat Exchanger Models

2.2.1 Pre-Heater and Vaporizer

The thermal design of shell and tube heat exchangers deserves a lot of attention, as the cost of heat exchangers, a major component of a power plant's capital cost, bears a direct relationship with the area of the heat transferring surface.

There are a number of available models for the thermal design of heat exchangers and the choice of the model depends on the purpose of the heat exchanger, i.e. preheater, vaporizer, superheater or any combination. For applications without phase change we refer to the Bell-Delaware or Kern method. The Kern method gives conservative results and is only suitable for preliminary sizing. The Bell-Delaware method is a very detailed method and is usually very accurate for estimating the shell-side heat transfer coefficient and pressure drop for commonly used tube arrangements [9].

If the shell and tube exchanger is to be used as a vaporizer then correlations pertaining to nucleate boiling, convective boiling and models providing a combination of the two all must be used. This is because the volume fraction of vapor increases to one as it rises towards the top-most tube row in the heat exchanger. The nucleate boiling models are an area of intense investigation in hope to achieve a fully mechanistic model in place of the empirical and semi-empirical models available in literature. Achieving a mechanistic model requires overcoming the uncertainties and complexities of the boiling phenomenon. This presents a complex [10] computational challenge.

In this paper the geothermal brine enters the vaporizer before entering the preheaters. The thermal design of the vaporizer is based on Aprin [11, 12] and Feenstra-Weaver-Judd method [13] for quality based void fraction calculations. The vaporizer's thermal design incorporates a row-wise calculation of heat transfer coefficients and void fraction, as the Aprin's Method combines different methods to calculate shell-side heat transfer coefficients depending on the void fraction. The geothermal brine leaving the vaporizer is fed to the preheater, whose thermal design is based on the Bell-Delaware method.

The vaporizer and preheater were both designed with common shell and tube parameters, which are listed in Table 3 and with the tube layout shown in Figure 3. To simplify the design, both heat exchangers are single pass heat exchangers. Longer shell and tube heat exchangers are more effective than large diameter heat exchangers; therefore, the shell diameter was limited to 450mm, which is standard pipe diameter to help reduce thickness and costs.[14]

Table 3 - Shell and Tube design parameters

Design Parameter	Value
Tube diameter D_o mm	25.4
Tube Thickness T_{th} mm	2.7
Tube Pattern	Triangular 30°
Tube Pitch Ratio	1.3

Shell internal diameter *Maximum without need for a rolled vessel*	450
Baffle Cut %	30
Tube Number	149
Tube Sheet Thickness	25
Tube to baffle clearance	0.8
Diameter of Tube bundle	404

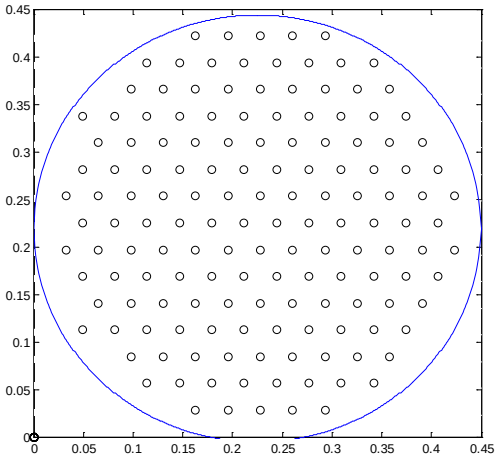

Figure 3 - Tube arrangement in the shell and tube heat exchangers

2.2.2 Air Cooled Condenser

ACCs are used in a number of ORCs in New Zealand and Table 4 lists the typical design parameters used for this ACC model.

Table 4 - Air Cooled Condenser design parameters

Design Parameter	**value**
Tube diameter D_o mm	25.4
Tube Thickness T_{th} mm	2.1
Fins per meter n_f fins/m	350
Fin Length F_L mm	16
Fin thickness F_{th} mm	1
Fin Material	Extruded Aluminum
Angular Pitch mm	50.8
Pitch	Triangular
Number of rows	3
Number of passes	1
Face Velocity V_{face} m/s	3.6
Fan Thickness mm	1
Max and Min Tube velocity – liquid m/s	2.7 – 1
Max and min Tube velocity – Gas m/s	30 – 15
Surface Roughness µm	45
Ambient Temperature °C	20
Air Cooler Type	Induced Draft

The first step was to analyze the air side heat transfer coefficient of the heat exchanger, which used equation 1 by Keller and Somers. An equation developed from the Briggs and Young correlations that cover a large range of air cooled heat exchangers [15].

Equation 1

$$h_a = K{G_{max}}^{0.681}/{D_o}^{0.319}$$

K is a constant 5.23 and G_{max} is the maximum mass flux of the air flowing through the heat exchanger, equation 2.

Equation 2

$$\boldsymbol{G_{max} = \rho V_{max}}$$

The maximum air velocity V_{max} is between the finned tubes and was calculated with equation 3 [15].The face velocity of the condenser is the recommended maximum 3.6m/s [8].

Equation 3

$$V_{max} = \frac{Pitch * V_{face}}{Pitch - D_o - 2(n_f)(F_L)(F_{th})}$$

The recommended maximum and minimum working fluid vapor and liquid velocities were used to determine the number of tubes in the heat exchanger. The tube side heat transfer was determined for both the superheated fluid and the condensing stage of the heat exchanger. Both sections use EES correlations to determine the heat transfer of the fluid flowing within a single pipe. The superheated fluid is a single phase flow within the pipe, and forced convection of internal pipe flow is used to determine the heat transfer for the de-superheating section.

The EES condensation procedure uses correlations by Dobson and Chato which have been experimentally validated by Smith et al [16]. There is some uncertainty in the heat transfer coefficient for very high pressure refrigerants, which could affect the results of an ACC with R134a. The condensing correlation averages heat transfer values of the condensing fluid at a number of discrete quality points and corresponding flow regimes. The fluid in the condenser is assumed to leave the condenser as a saturated liquid with no sub-cooling.

2.2.3 Costing

A basic costing analysis was done for each heat exchanger. The heat exchanger hand book has a guide for basic heat exchanger costing for both heat exchanger types [14]. The costing analysis for a shell and tube heat exchanger accounts for shell length and diameter, shell and tube pressure, and material choice, which was chosen to be carbon steel with no impact on the costing. The ACC cost estimate takes into account tube number, length, thickness, number of rows, fin type, fan size, and pressure.

3. RESULTS AND DISCUSSION

The following section has the results of the ORC and the details from the heat exchanger analysis that can help with working fluid selection.

3.1 ORC Results for a 250 kW ORC with a 130°C heat source

The ORC was modeled so that each fluid would produce a net output of 250 kW from a 130°C geothermal resource.

Table 5 – 130°C ORC Working fluid flow rate and parasitic loads

Working Fluid	$\eta_{thermal}$ %	Feed Pump Load kW	Work loss from pressure losses kW	$\dot{m}_{wf}$ kg/s
N-Pentane	5.84	5.6	0.14	11.6
R245fa	5.90	12.1	0.24	24.3
R134a	3.31	46.3	2.45	64.6
Isopentane	5.90	7.3	0.31	12.3
Isobutane	6.09	25.7	1.02	14.7

Table 6 – Geothermal flow rate and condenser Parasitic Loads

Working Fluid	$\dot{m}_{geo}$ kg/s	Tout Geo °C	ACC		WCC	
			$\dot{m}_{air}$ kg/s	Load kW	$\dot{m}_{water}$ kg/s	Load kW
N-Pentane	34.3	99.94	136.6	3.8	32.89	1.32
R245fa	34.0	99.25	138	3.8	33.41	1.34
R134a	47.5	85.45	288.1	7.9	69.37	2.77
Isopentane	33.8	99.59	136.1	3.7	32.77	1.31
Isobutane	33.8	98.37	141.7	3.9	34.12	1.36

Table 5 and 6 are the results of the ORC model which show the outlet temperature of the geothermal fluid from the ORC as well as the corresponding working fluid and geothermal fluid mass flow rates. The fluid mass flow rates are also key parameters affecting the parasitic loads on the system. Each ORC produces a net power of 250 kW after the feed pump losses but excluding the required power for the condenser fans.

The evaporator pressure of R134a was limited by the maximum allowable pressure of the system. ORCs researched in literature generally do not operate above 25 bar and so this was set as the maximum operating pressure of the ORC. A system above 25 bar would require a machined turbine housing [17], which is more expensive than a cast option. R134a also requires 3 degrees of superheat to ensure it leaves the turbine as a dry superheated vapor and avoid droplet formation during expansion.

3.1.1 Vaporizer Results

Table 7 - Results from the Vaporizer

T=130	Length	Duty kW	Tout °C
N-Pentane	6.13	3557	104.3
R245fa	5.20	3479	104.5
R134a	7.48	7532	90.4
Isopentane	5.70	3507	104.2
Isobutane	4.65	3387	105.0

The results of the detailed vaporizer analysis show that the working fluid does impact the length of the heat exchanger; however, this is more likely due to the difference in heat duty. The largest vaporizer is required for R134a and this also requires the largest quantity of heat transfer in the vaporizer. Understanding the length of the required heat exchanger can help select the appropriate working fluid for a compact ORC.

3.1.2 Preheater

Table 8 - Results from the preheater

T=130	Length	ΔP Pa	Tout °C	Duty kW
N-Pentane	2.70	54	98.6	818
R245fa	2.75	108	97.7	962.9
R134a	4.95	1068	83.1	1425
Isopentane	3.05	50.09	98.1	868
Isobutane	4.5	112	96.8	1149

There are similarities between the preheater and vaporizer results and as expected the fluid with largest required duty has the largest heat exchanger. An exception to this is Isopentane, which has smaller duty compared to R245fa; however, requires a larger preheater. The other important aspect of a preheater is the pressure losses on the shell side as this impacts the performance of the ORC. The work loss from the pressure losses of all heat exchangers in the ORC is shown in table 5.

3.1.3 Condenser

Two important aspects from the ACC results are the pressure drop experienced by the fluid as this increases the work load on the pump and the overall size. R134a requires the most cooling for the ORC, which in turn requires the largest heat exchanger. R134a is a dense fluid and so the volumetric flow ratio was low compared to the other working fluids, which limited the number of tubes in the heat exchanger, increasing the required length. Increasing the tube number does decrease the overall length; however, it will also reduce the effectiveness as the fluid velocity within the tube decreases [18].

Table 9 - Results of the ACC

T=130	Length	Face m^2	ΔP Pa	Duty kW
N-Pentane	8.25	31.6	5018	4126
R245fa	11.19	35.7	10193	4191
R134a	19.06	64.9	31404	8703
Isopentane	10.95	30.1	12240	4111
Isobutane	19.21	30.8	32712	4280

3.2 ORC Results for a 250 kW ORC with a 100°C heat source

An important consideration for an ORC is how changes to the resource temperature may affect the ORC. The following results are of an ORC maintaining the required 250kW net output from a 100°C resource.

Table 10 - 100°C ORC Working fluid flow rate and parasitic loads

Working Fluid	$\eta_{thermal}$ %	Feed Pump Load kW	Work loss from pressure loss kW	$\dot{m}_{wf}$ kg/s
N-Pentane	2.5	4.7	0.49	28.56
R245fa	2.6	9.9	4.3	59.11
R134a	2.7	43.9	7.1	79.14
Isopentane	2.6	6.2	0.84	30.25
Isobutane	2.6	21.3	2.52	35.62

Table 11 – Geothermal flow rate and condenser Parasitic Loads

Working Fluid	$\dot{m}_{geo}$ kg/s	Tout Geo °C	ACC		WCC	
			$\dot{m}_{air}$ kg/s	Load kW	$\dot{m}_{water}$ kg/s	Load kW
N-Pentane	220.5	89.22	323.1	8.9	77.82	3.1
R245fa	221.8	89.14	327.5	9.0	78.87	3.2
R134a	220.2	88.27	355	9.7	85.5	3.4
Isopentane	217.8	89.17	320.5	8.8	77.17	3.1
Isobutane	223.5	89.03	333.7	9.2	80.35	3.2

The resulting ORC requires much higher flow rate for both the geothermal fluid and the working fluid. The reduced geothermal temperature reduces the evaporation temperature of the system and consequently reduces the specific enthalpy drop in the turbine, as the condensing temperature is still high in an attempt to minimize the ACC cost. The reduced enthalpy drop requires higher working fluid mass flow rates to maintain the desired 250kW output of the ORC. The increased working fluid mass flow rate is directly related to the heat duty of the system which increases the required geothermal fluid mass flow rate. Realistically, geothermal flow rate may not be able to be increased and so, with the same flow rate as 130°C resource the net power output would roughly be 38kW.

3.2.1 Vaporizer Results

The following sections show how the reduced temperature would require significantly larger heat exchangers to maintain the same power output. The implications of this are that a significant investment must be made in heat exchangers to build redundancy and flexibility into an ORC.

Table 12 – Results of the Vaporizer

T=100	Length	Duty kW	Tout °C
N-Pentane	19.60	9251	89.67
R245fa	14.00	9246	89.5
R134a	10.70	9617	89.11
Isopentane	19.10	9139	89.47
Isobutane	11.75	9310	89.4

3.2.2 Preheater

Table 13 – Results of the Pre Heater

T=100	Length	ΔP Pa	Tout °C	Duty kW
N-Pentane	1.8	269	88.81	782
R245fa	1.8	529	88.53	897
R134a	3.15	1312	87.62	1370
Isopentane	1.98	258	88.56	825
Isobutane	2.73	529	88.32	1047

3.2.3 Condenser

Table 14 - Results of the Condenser

T=100	Length	Face m^2	ΔP Pa	Duty kW
N-Pentane	9.66	74.8	8679	9763
R245fa	19.55	72.9	79287	9894
R134a	25.55	75.3	84815	10726
Isopentane	11.49	73.4	13834	9682
Isobutane	19.15	74.7	31102	10080

3.3 ORC Results for a 250 kW ORC with a reduced condensing temperature

It is unusual to operate an ORC at an elevated condensing temperature with the goal of reducing the cost of the ACC because a lower condensing temperature greatly improves ORC performance. Table 15 and 16 are the results of an ORC running at a more reasonable condenser temperature, below 40°C. This ORC requires less geothermal fluid to achieve the required 250kW when the geothermal temperature can be reduced further. The decreased condensing temperature also increases the size and work required by the ACC.

Table 15 – ORC performance at a reduced condenser temperature

Fluid	$\eta_{thermal}$ %		Feed Pump Load kW		$\dot{m}_{geo}$ kg/s	
	130C	100C	130C	100C	130C	100C
N-Pentane	8.9	6.1	3.0	2.4	12.9	33.2
R245fa	9.2	6.2	6.1	4.7	12.4	32.5
R134a	9.5	6.4	25.8	19.4	11.6	31.9
Isopentane	9.0	6.1	3.9	3.1	12.7	32.9
Isobutane	9.3	6.2	13.6	10.9	12.3	32.4

Table 16 - ORC results - Geothermal outlet temperature and ACC area

Fluid	Geothermal Outlet Temp °C		ACC Face Area m^2		ACC fan work kW	
	130°C	100°C	130°C	100C	130C	100C
N-Pentane	78.0	70.5	65.98	99.10	7.3	11.4
R245fa	76.8	69.7	75.45	64.51	7.3	11.4
R134a	70.5	68.8	78.06	133.7	8.1	11.8
Isopentane	77.5	69.9	61.98	97.72	7.2	11.3
Isobutane	75.5	69.3	64.74	117.4	7.3	11.5

3.4 Cost Breakdown

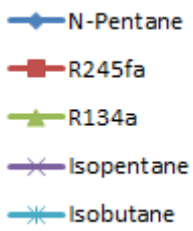

Figure 4 – Legend for figures 5 and 6

A cost analysis was conducted for the heat exchangers which can be used to estimate the most economical working fluid choice. The cost of the heat exchangers was normalized to the size of the ORC to give the cost of all the heat exchangers in the ORC per kW of output power. All costs are calculated in USD.

The reduction in condensing temperature significantly impacts the ACC but not the pre-heater and vaporizer costs. An ORC operating with a low temperature condenser will cost more as the surface area required for the ACC increases between 40% - 90% as the condensing temperature is reduced. The reduced condensing temperature, however, does increase the performance of the ORC. Figure 5 shows the average cost of all heat exchanger equipment in an ORC for each working fluid at the two operating points. It is clear that at the low temperature range some savings can be made by selecting an appropriate working fluid. R134a operates at the highest pressure of the fluids, which contributes to the higher cost of R134a. N-Pentane and Isopentane both have the lowest cost per kW in figure 5 over the two temperatures investigated and this could suggest why N-Pentane and Isopentane is the working fluid typically used in Ormat ORCs. Figure 7 also supports Ormats use of pentane in ORCs as it has the best capital cost to surface area ratio of all the fluids investigated.

The rough market cost for an ORC for a 100°C and 130°C resource is 7000$/kW and 4500$/kW respectively[19]. The results of the heat exchanger costing show that a significant portion of this cost comes from the heat exchanges; therefore, intelligent heat exchanger design and manufacture is key to an ORC's success.

Figure 6 uses equation 4, the basic heat exchanger equation, to determine the required heat transfer area of the heat exchanger. The costs were normalized with the ORC output as well.

Equation 4

$$A = \frac{Q}{U(LMTD)}$$

The surface area is the most common initial cost estimate for a heat exchanger. The average estimates of \$500m^2 and \$600/m^2 for the vaporizer and condenser respectively[20] were used to compare with results of this paper. There is no significant cost difference for each working fluid using this approach.

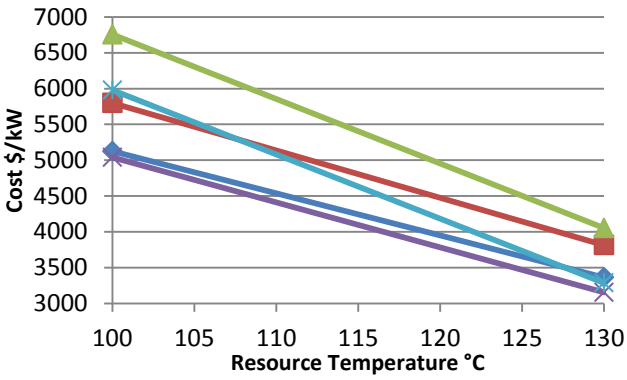

Figure 5 – Average cost using detailed approach to Heat Exchanger design

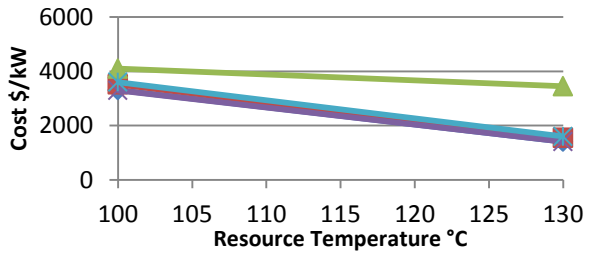

Figure 6 – Average cost using simple approach to Heat Exchanger design

The costing analysis shows that a more extensive heat exchanger analysis can help with working fluid selection. The impact is enhanced as the resource temperature decreases.

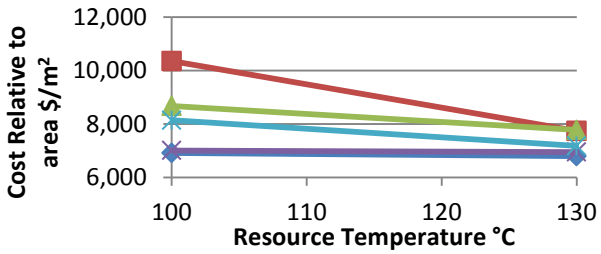

Figure 7 - Heat Exchanger cost per unit area of heat transfer

4. CONCLUSION

The results of modeling heat exchangers with a number of working fluids show that the working fluids do impact the design and cost of the heat exchanger. Their impact on the overall cost of the heat exchangers is enhanced at lower resource temperatures. The cost of traditional heat exchangers at the low temperature range could encourage the use of alternative heat exchangers typically not used in geothermal ORCs, such as plate type heat exchangers.

The working fluid selection process would benefit from a detailed heat exchanger analysis. However, the fluids which result in a more costly heat exchanger generally don't perform as well in the thermodynamic cycle analysis; therefore, initial working fluid screening from the ORC results should eliminate these fluids from the working fluid options.

ACKNOWLEDGEMENTS

This work is part of the Above Ground Geothermal and Allied Technology (AGGAT) Program supported with funding from the NZ Ministry for Business Innovation and Employment contract: HERX1201 administered through the Heavy Engineering Research Association (HERA). Special thanks to Sandeep Siwach for his shell and tube heat exchanger models and knowledge.

REFERENCES

1. Kestin, J., et al., *Sourcebook on the production of electricity from geothermal energy*, 1980, Brown Univ., Providence, RI (USA).
2. Watanabe, C. *IHI Expects Japan Market for Small Geothermal Projects to Expand*. 2014.
3. Dipippo, R., *Personal Communication - Binary Plant Design*, 2013.
4. Legmann, H. and P. Sullivan. *The 30 MW Rotokawa I geothermal project five years of operation*. in *International Geothermal Conference*. 2003.
5. Brasz, J.J., B.P. Biederman, and G. Holdmann. *Power production from a moderate-temperature geothermal resource*. in *GRC annual meeting, Reno, Nevada*. 2005.
6. Schochet, D.N. *Case histories of small scale geothermal power plants*. in *Proceedings of the 2000 World Geothermal Congress*. 2000.
7. DiPippo, R., *Second Law assessment of binary plants generating power from low-temperature geothermal fluids*. Geothermics, 2004. **33**(5): p. 565-586.
8. Perry, R.H., D.W. Green, and J.O. Maloney, *Perry's chemical engineer's handbook*, in *Perry's chemical engineer's handbook*. 1984, McGraw-Hill Book.
9. Ozden, E. and I. Tari, *Shell side CFD analysis of a small shell-and-tube heat exchanger*. Energy Conversion and Management, 2010. **51**(5): p. 1004-1014.
10. Chu, H. and B. Yu, *A new comprehensive model for nucleate pool boiling heat transfer of pure liquid at low to high heat fluxes including CHF*. International Journal of Heat and Mass Transfer, 2009. **52**(19): p. 4203-4210.
11. Aprin, L., P. Mercier, and L. Tadrist, *Local heat transfer analysis for boiling of hydrocarbons in complex geometries: a new approach for heat transfer prediction in staggered tube bundle*. International Journal of Heat and Mass Transfer, 2011. **54**(19): p. 4203-4219.
12. Aprin, L., P. Mercier, and L. Tadrist, *Experimental analysis of local void fractions measurements for boiling hydrocarbons in complex geometry*. International journal of multiphase flow, 2007. **33**(4): p. 371-393.
13. Feenstra, P., D. Weaver, and R. Judd, *An improved void fraction model for two-phase cross-flow in horizontal tube bundles*. International Journal of Multiphase Flow, 2000. **26**(11): p. 1851-1873.
14. Hewitt, G.F. and J. Barbosa, *Heat exchanger design handbook*. Vol. 98. 2008: Begell House.
15. Shah, R.K., E.C. Subbarao, and R.A. Mashelkar, *Heat transfer equipment design*. 1988: CRC Press.
16. Nellis, G. and S.A. Klein, *Heat transfer*. 2009, New York: Cambridge University Press.
17. ISO, *ISO 14661:2000 Thermal Turbines for Industrial applications (Steam turbines, Gas expansion turbines) -- General Requirements*, 2000, ISO: Switzerland.
18. Exchangers, D.H. *Tube Velocity in Heat Exchangers*. 2004 [cited 2014 29/8/14]; Available from: http://deltathx.com/uploadsDocs/Tube%20Velocity%20in%20Heat%20Exchangers.pdf.
19. IRENA. *Geothermal Cost Charts*. 2014 14/10/2014]; Available from: http://costing.irena.org/charts/geothermal.aspx.
20. Nazif, H., *Feasibility of developing binary power plants in the existing geothermal production areas in Indonesia*. United Nations University Geothermal Program, 2011. **Report 29**: p. 709-735.